Effect of Soil-Structure Interaction on the Seismic Response of Existing Low and Mid-Rise RC Buildings

Ibrahim Oz [1,*] , **Sevket Murat Senel** [2,*], **Mehmet Palanci** [3] **and Ali Kalkan** [2]

1   Department of Civil Engineering, Kirsehir Ahi Evran University, 40100 Kirsehir, Turkey
2   Department of Civil Engineering, Pamukkale University, 20160 Pamukkale, Turkey; akalkan@pau.edu.tr
3   Department of Civil Engineering, Istanbul Arel University, 34537 Istanbul, Turkey; mehmetpalanci@arel.edu.tr
*   Correspondence: ibrahim.oz@ahievran.edu.tr (I.O.); smsenel@pau.edu.tr (S.M.S.)

Abstract: Reconnaissance studies performed after destructive earthquakes have shown that seismic performance of existing buildings, especially constructed on weak soils, is significantly low. This situation implies the negative effects of soil-structure interaction on the seismic performance of buildings. In order to investigate these effects, 40 existing buildings from Turkey were selected and nonlinear models were constructed by considering fixed-base and stiff, moderate and soft soil conditions. Buildings designed before and after Turkish Earthquake code of 1998 were grouped as old and new buildings, respectively. Different soil conditions classified according to shear wave velocities were reflected by using substructure method. Inelastic deformation demands were obtained by using nonlinear time history analysis and 20 real acceleration records selected from major earthquakes were used. The results have shown that soil-structure interaction, especially in soft soil cases, significantly affects the seismic response of old buildings. The most significant increase in drift demands occurred in first stories and the results corresponding to fixed-base, stiff and moderate cases are closer to each other with respect to soft soil cases. Distribution of results has indicated that effect of soil-structure interaction on the seismic performance of new buildings is limited with respect to old buildings.

Keywords: soil-structure interaction; nonlinear analysis; direct time history analysis; existing buildings; seismic performance

1. Introduction

The determination of the seismic performance of existing buildings has gained very much interest in recent years, and today there are a greater number of specifications and regulations containing provisions on this issue [1]. The seismic behavior of a building is directly related to the interaction between the three interconnected systems, which are superstructure, foundation and soil medium surrounding the foundation system [2]. Advances and experiences in earthquake engineering, reconnaissance surveys after strong earthquakes and academical studies about soil-structure interaction (SSI) have shown that old buildings designed by limited knowledge are far from meeting the current standards and performance objectives of new designs. Although there were studies in literature suggesting the use of force-based computational approaches for the modeling of SSI [3], the application of these methods has been very limited, and they have not found significant use in practice [1].

Particularly over the last two decades the widespread use of displacement-based methods, which include nonlinear calculations such as static pushover analysis, provide to investigate SSI beyond the elastic limits [3,4]. Realistic estimations of both displacement capacities and seismic drift demands became possible by using nonlinear analysis methods. The damage observations and detailed structural analyses have shown that SSI could significantly alter both the capacity and demand-related

structural parameters (e.g., vibration period, drift capacity, etc.) and hence the seismic performance of buildings [5,6]. All these observations and findings have shown that SSI effects should be considered necessary for the design and assessment of buildings.

Earlier studies of SSI contained complex arithmetic formulas relating to wave propagation in several directions [1], and this approach made these studies difficult to comprehend. SSI is not covered in the undergraduate level and therefore, it is difficult for many engineers to apply these methods in design phase. While regulations and documents about SSI are available for engineers in countries such as USA [7], these sources have guided earthquake engineers only to a limited extent. In many countries, there are still no mandatory code regulations and directions that enforce the engineers to consider the SSI effects in design and assessment of buildings.

SSI analyses are performed to investigate the effect of various soil conditions on the response of structures under seismic actions. There are two approaches for the calculation of SSI, namely the "direct" and "substructure" methods [8]. In the direct method, the structure and soil are modeled within a single finite element network in which the nonlinearities of the superstructure and the soil are represented as a whole, and structure and soil are analyzed together. On the other hand, direct method requires considerable calculation efforts and analysis duration, and therefore, it is not suitable when assessing a lot of buildings, as in the case of this study. The combined use of nonlinear time history analysis and direct method makes this situation more complicated. In the "substructure method," on the other hand, the soil and the structure are considered as distinct systems. The behavior of the foundation and soil is represented by dynamic stiffness and damping coefficients and the effect of interaction between the soil and foundation is transmitted to the structure by means of dashpots and springs. This method considerably shortens the duration of analysis since the soil is not modeled directly. It is thus more favorable to use the substructure method in the studies when dealing with a large number of buildings. In this study, a lot of buildings (40 buildings) were considered and seismic response of these buildings under various soil conditions was investigated by using nonlinear time history analyses. Therefore, substructure method is preferred to investigate effect of SSI by considering the required efforts. Academical studies considering the SSI have increased in the United States towards the end of the 2000s and some of them were summarized in the FEMA-440 report [3]. In this report, regulations and expressions are presented to explain how SSI can be considered in nonlinear static analyses. The findings of these studies were also included in US code specifications [4]. However, the expressions in FEMA-440 [3] and the ASCE-2007 [4] regulations are not recommended for nonlinear time history analyses and therefore this situation required new studies on this subject. The results of subsequent studies related with the SSI in performance-based earthquake engineering were summarized in 2012 and the method which can be used in non-linear time history analysis was proposed [1]. This approach was also used in this study during the analyses of selected building models and SSI was represented based on the expressions taken from these studies.

There are many other studies addressing the non-building type of structures in the literature. Gazetas [9] proposed algebraic formulas and tables that could be used to calculate the dynamic properties of foundations of different shapes. Mylonakis and Gazetas [6] discussed whether SSI effects could be beneficial for structures. They have compared the seismic behavior of structures calculated by using traditional methods and by considering SSI effects. The authors showed that an increase in the natural vibration period may not always lead to a lower spectral acceleration response and noted that this may result in an unsafe structural assessment. Mylonakis et al. [10] studied the seismic analysis and design of bridge piers and proposed simple expressions for the calculation of kinematic effects. Fatahi et al. [11] examined the seismic performance of empirical buildings with SSI and showed that the seismic performance of buildings varied significantly depending on the soil conditions. Shehata et al. [5] investigated the variations in SSI effects depending on the use of different demand calculation methods in multi-story buildings. Their research has shown that seismic performance evaluations are not within the reliable limits if the effects of SSI are ignored. Increasing number of academical studies and engineering reports imply that in the next generation codes SSI modeling

will necessarily be required and consideration of SSI effects in design will be mandatory. However, buildings constructed before these findings will still be the weak point of the cities that are prone to seismic risk.

Turkey is an earthquake-prone country and the majority of existing building stock, which consist of low and mid-rise reinforced concrete (RC) buildings, were designed without considering SSI. Therefore, the main purpose of the present study is to investigate the effects of SSI on the seismic response of existing buildings. For this purpose, 40 RC buildings selected from Turkey were investigated. TEC-2007 [12] and TBEC-2018 [13] include the regulations which define the seismic performance assessment of existing buildings. However, both Turkish earthquake codes do not comprise the definitions or formulations which explain how to model SSI in design and assessment.

In this study, residential RC buildings that constitute three-, four-, five- and six-story buildings were selected, and they were mainly classified into two groups as "old" and "new" buildings according to their construction dates [14]. TEC-1998 [15] is accepted as the reference code to distinguish buildings since this code applied the capacity design principle at the first time and considerably increased the design forces and limited the displacement demands in terms of drift ratios. This situation significantly differs the strength and stiffness capacity of existing buildings constructed before and after TEC-1998 in Turkey. Moreover, mandatory building control law, earthquake insurance and improvements in the workmanship and material qualities after the 1999 Marmara earthquakes increased the safety of newer buildings with respect to old ones.

Design projects of these new and old buildings (20 new, 20 old) were obtained from the municipality archives in Denizli city. Moment-curvature analyses were performed for beams and columns and member damage limits were determined by using the strain-based definitions of Turkish Earthquake Code. Both 2007 and 2018 codes use the strain base damage assessment and, in both codes, ultimate concrete compression strain (which is the major parameter that controls damage capacity of the RC members) is limited to 1.8%. Non-linear building models were obtained by assigning the plastic hinges to the critical sections of RC members. Capacity curves of inelastic building models were obtained by using static pushover analyses and drift demands were calculated by using non-linear time history analyses.

In fact, the aim of this study is not to evaluate or compare the non-linear modeling rules or assumptions of any codes. The main objective of this study is to investigate and compare the effect of SSI on the seismic capacity and demand calculations of existing buildings constructed on the various soil conditions changing from stiff to soft. The main idea is to compare building capacity curves, inelastic deformation demands, inter-story drift demands and overall seismic response of existing buildings which have different story numbers, different stiffness and strength capacities, and different soil conditions.

For this purpose, four different soil conditions were considered. Response of buildings under fixed-base, stiff, moderate and soft soil cases were investigated. As mentioned previously, the "Substructure Method" was employed to explore the effects of the SSI. In order to determine the seismic demand generated by buildings on different soil conditions, 20 acceleration records selected from major earthquakes were used. Accordingly, 3200 dynamic nonlinear time history analyses (40 buildings, 4 different soil profiles and 20 acceleration records) were performed for three-dimensional multi-story buildings models. Additionally, nonlinear static pushover analyses were carried out to identify the effect of SSI on the capacity curves of selected buildings and the results were compared.

2. Nonlinear Modeling of Existing Buildings

The majority of existing residential building stock of Turkey is composed of low and mid-rise RC buildings. Therefore, in this study buildings were selected to reflect this situation and story numbers of selected existing buildings vary between three and six. In the study, buildings were grouped according to their story numbers and construction dates and each story group has five buildings. Distribution of

the story numbers and construction dates of selected buildings are presented in Table 1. It should be stated that construction date of buildings has a crucial role since improvements in the workmanship and material qualities increased the safety of new buildings. In both seismic codes, a force-based design approach was used. However, capacity design principles were not considered in TEC-1975. One of the most important differences between the codes is also that TEC-1998 enforced the use of "ultimate strength design" for the analysis and design of RC cross-sections and this method is essential for the application of capacity design principles. In TEC-1975, design spectrum was not defined, but lateral seismic forces were calculated according to earthquake zone coefficient (C_o), seismic weight (W), structural configuration system type (K), soil condition (S) and importance factor (I). Maximum lateral force demand was recommended as 10% of seismic weight for the design of structures ($C_o = 0.1$). In both seismic codes, soil conditions were only considered to calculate corner periods of the spectrum. Minimum allowable concrete strength was equal or higher than 16 MPa in TEC-1975, but this value was increased to 20 MPa in TEC-1998. In TEC-1975, S220 steel class which has a yield strength of 220 MPa was allowed, but in TEC-1998, minimum S420 steel which has a yield strength of 420 MPa was recommended. It can be said that new buildings have a greater stiffness, strength and ductility capacity with respect to old buildings. By using such kind of classification, it is aimed to investigate the effect of SSI on the new (98+) and old buildings (98−).

Table 1. Number of old and new existing buildings for which a soil-structure interaction (SSI) model has been developed.

Number of Stories	Old Buildings (98−)	New Buildings (98+)
3	5	5
4	5	5
5	5	5
6	5	5

The structural properties of buildings, such as section dimensions, reinforcement details, material properties, dead and live loads acting on the buildings were determined according to their design projects. Investigation of RC design projects have revealed that concrete strength of old buildings is mainly 16 MPa, and design projects of these buildings have shown that S220 steel class with a yield strength (f_y) of 220 MPa is used for both longitudinal and transverse reinforcement. It was also observed that stirrups were not used in the cross-section of members, and transverse reinforcement spacing of the members was mainly 200 mm and this was even inadequate according TEC-1975 design rules. Furthermore, design projects of buildings have shown that section dimensions of the columns were reduced in the upper stories. Buildings designed according to TEC-1998 or higher have identical steel class (S420) which yield strength is 420 MPa. However, concrete strengths were changed from project to project. For this reason, concrete strength of new buildings is not identical, and they were modeled according to their own concrete strengths. It was also observed that confinement details of code provisions were applied to beam and columns in new buildings. In addition, column dimensions were not reduced along the building height. In Figure 1 shows some pictures from the design projects of a sample four-story building and a photo from field investigation is shown.

Strength and deformation capacities of members at critical sections were determined via moment-curvature analyses. Stress-strain behavior of confined concrete was represented by Modified Kent-Park model [16]. Since the purpose of the study is concentrated on the capacity and seismic demand estimation of buildings, intermediate damage limits (Immediate Occupancy and Life Safety) of structural members were not used. Collapse limits of members were obtained according to the strain-based damage definition given in Equation (1). In this equation, limits were calculated depending on the compression strains of confined concrete (ε_{cc}) and tensile strain (ε_s) of steel. Compression strain regarding collapse limit is formulated by the amount of transverse reinforcement. In the equation, confined concrete strain limits are expressed depending on the ratio of existing (ρ_s) to required (ρ_{sm})

volumetric transverse reinforcement ratio of members. While performing moment-curvature analyses, both elongation in steel and compression in concrete were checked and collapse limit was determined according to whichever came first. In other words, minimum curvature values were determined from both expressions as indicated in Equation (1). In addition to flexural capacity of beams and columns, shear capacity of members was also checked for the possible shear failure of RC members [17].
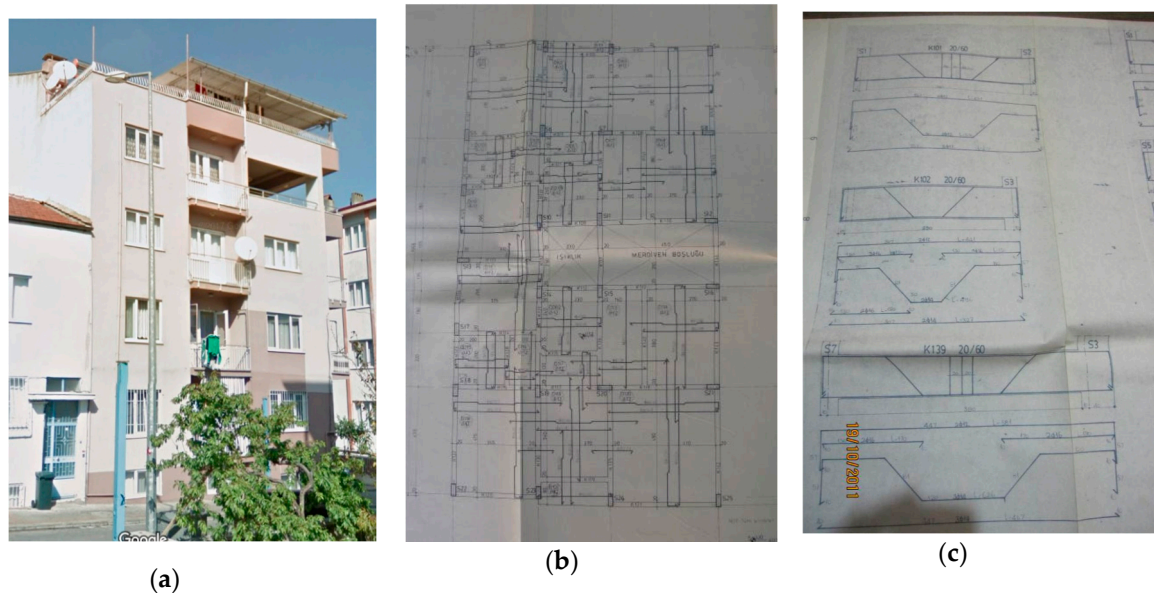

Figure 1. Field investigations and photos of design projects ((**a**): Building picture, (**b**): Plan of building, (**c**): reinforcement details in the RC project).

$$\phi_{collapse} = min\left[\phi@\left(\varepsilon_{cc} = 0.004 + 0.014\left(\frac{\rho_s}{\rho_{sm}}\right) \le 0.018\right); \phi@(\varepsilon_s = 0.06)\right] \qquad (1)$$

3. SSI Modeling of Selected Buildings

The effect of SSI is much more significant in low-rise and stiffer buildings with respect to high-rise long period structures [1]. Buildings considered in this study are not high-rise structures, and therefore it is expected that SSI would alter the response of examined buildings. The existing Turkish earthquake code regulations do not require engineers to consider SSI effects, whether designing new buildings or determining the seismic performances of existing buildings. Instead, the regulations mentioned above recommended the "Fixed-Base Approach" for both design and evaluation of buildings. As mentioned before, the primary aim of this paper is to determine SSI effects on the superstructures by considering the "Substructure Method." Details of the substructure method can be found in the literature [8,18].

"Inertial Interactions" and "Kinematic Interactions" are two components, and they should be considered in modeling of structures according to substructure method. Inertial interaction refers to the displacements and rotations occurring at the foundation level of the superstructure due to shear and moment related effects. A schematic illustration of deformations for single degree of freedom system (SDOF) caused by the lateral forces is shown in Figure 2. As a result of this interaction, an elongation of the natural vibration period of the structure is expected. Accordingly, this situation may have a dramatic effect on the seismic response of the structure. The ratio vibration periods of fixed base to SSI system for SDOF system can approximately be calculated by Equation (2).

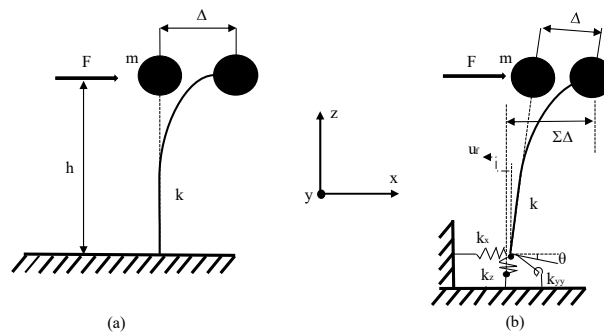$$\frac{T'}{T} = \sqrt{1 + \frac{k}{k_z} + \frac{kh^2}{k_{yy}}} \qquad (2)$$

Figure 2. Typical lateral deformation of single degree of freedom system (SDOF) model according to (**a**) fixed base, (**b**) SSI system.

In Equation (2), T' denotes the elongated period, k is the stiffness of the structure, k_z is the stiffness of the vertical spring, h is the effective modal height, which can be taken as two-thirds of the structure height, and k_{yy} is the stiffness of the rotational spring about the y-axis.

On the other hand, kinematic interaction defines the reduction in free-field ground motions at the base due to stiff foundation elements located on or inside the soil medium. The variation between free-field and foundation input motion (U_{FIM}) is expressed by a transfer function representing the ratio of foundation to free-field motion. Two components cause these reductions. The first one is the "Base Slab Averaging" which defines transition of spatially variable ground motions from soil medium to foundation due to the stiffness and strength changes caused by the foundation system [1]. The second one is the "Embedment Effects" in which foundation level motions are reduced because of ground motion reduction along the depth of the foundation. In the present study, three different soil types were examined, namely stiff, moderate, and soft. It should be noted that soil types are not classified as A, B or D as described in the majority of seismic codes, they are only used to represent different soil characteristics. Mean shear wave velocities (V_{s30}) corresponding to these soil types in each direction are given in Table 2 [19,20]. Selected V_{s30} values are determined according to study of (Pitilakis et al., 2013). Shear modulus of these soil conditions were calculated by using Equation (3). In this equation, V_s defines the shear wave velocity of soil, G denotes the soil shear modulus, and ρ_s denotes the soil mass density. The mechanical properties such as mass densities and Poisson's ratios of soils used in this study are given in Table 3.

$$V_s = \sqrt{\frac{G}{\rho_s}} \tag{3}$$

Table 2. Mean shear wave velocities for considered soils types.

Shear Wave Velocities (Mean V_{s30})	Stiff	Moderate	Soft
Horizontal displacement (x) (m/s)	720	285	180
Horizontal displacement (y) (m/s)	900	360	224
Vertical displacement (z) (m/s)	720	285	180
Rotation about x-axis (xx) (m/s)	1020	405	255
Rotation about y-axis (yy) (m/s)	1080	430	270
Torsion about z-axis (zz) (m/s)	1020	405	255

Table 3. Mass densities (ρ_s) and Poisson's ratio of soil types.

	Stiff	Moderate	Soft
Mass density (ρ_s) (KN/m^3)	22	20	18
Poisson's ratio (γ)	0.25	0.33	0.42

Modeling of buildings according to the substructure method is essentially performed in two parts. In the first part, the motion of the massless foundation system is calculated without the presence of the superstructure. The second part consists of the application of motion to the structure where soil properties are simulated by a group of equivalent springs and dashpots [21,22]. Equivalent soil properties of the foundation-soil interface are represented with springs and dashpots. The stiffness and damping of these springs and dashpots were calculated according to equations proposed by Pais and Kaussel [18]. In the present study, stiffer springs (k_2, k_3, k_4), which were calculated as a function of interior springs (k_z^i) and the stiffness intensity modifiers ($R_{k,xx}$–$R_{k,yy}$) along the foundation edges (R_eL and R_eB), are used to prevent the underestimation of rotational stiffness (Figure 3). Consequently, the total stiffness of the foundation was determined. The symbols "L" and "B" represent the dimension of the foundation system and they are taken as half of the actual dimensions. R_e is the foundation end length ratio which can be taken between 0.3 and 0.5. Damping intensities of dashpots (Figure 3, c_z^i) along the foundation edges were reduced by a damping intensity modifier ($R_{c,xx}$–$R_{c,yy}$) to not overestimate the foundation rotational damping (c_2, c_3, c_4). A schematic illustration of link and dashpot assignments to the foundation-soil interface is shown in Figure 3

$$k_z^i = \frac{k_z}{4BL} \quad c_z^i = \frac{c_z}{4BL}$$

$$k_2 = R_{kxx}*k_z*d_A$$
$$c_2 = R_{cxx}*c_z*d_A$$
$$k_3 = R_{kyy}*k_z*d_A$$
$$c_3 = R_{cyy}*c_z*d_A$$
$$k_4 = (k_2+k_3)/2$$
$$c_4 = (c_2+c_3)/2$$

Mean of edge L and edge B spring/dashpots

$$R_{k,xx} = \frac{\left(\frac{3k_{xx}}{4k_z^i B^3 L}\right) - (1 - R_e)^3}{1 - (1 - R_e)^3}$$

$$R_{c,xx} = \frac{\frac{3c_{xx}}{4c_z^i B^3 L}}{R_{k,xx}(1 - (1 - R_e)^3) + (1 - R_e)^3}$$

$$R_{c,yy} = \frac{\frac{3c_{yy}}{4c_z^i B^3 L}}{R_{k,yy}(1 - (1 - R_e)^3) + (1 - R_e)^3}$$

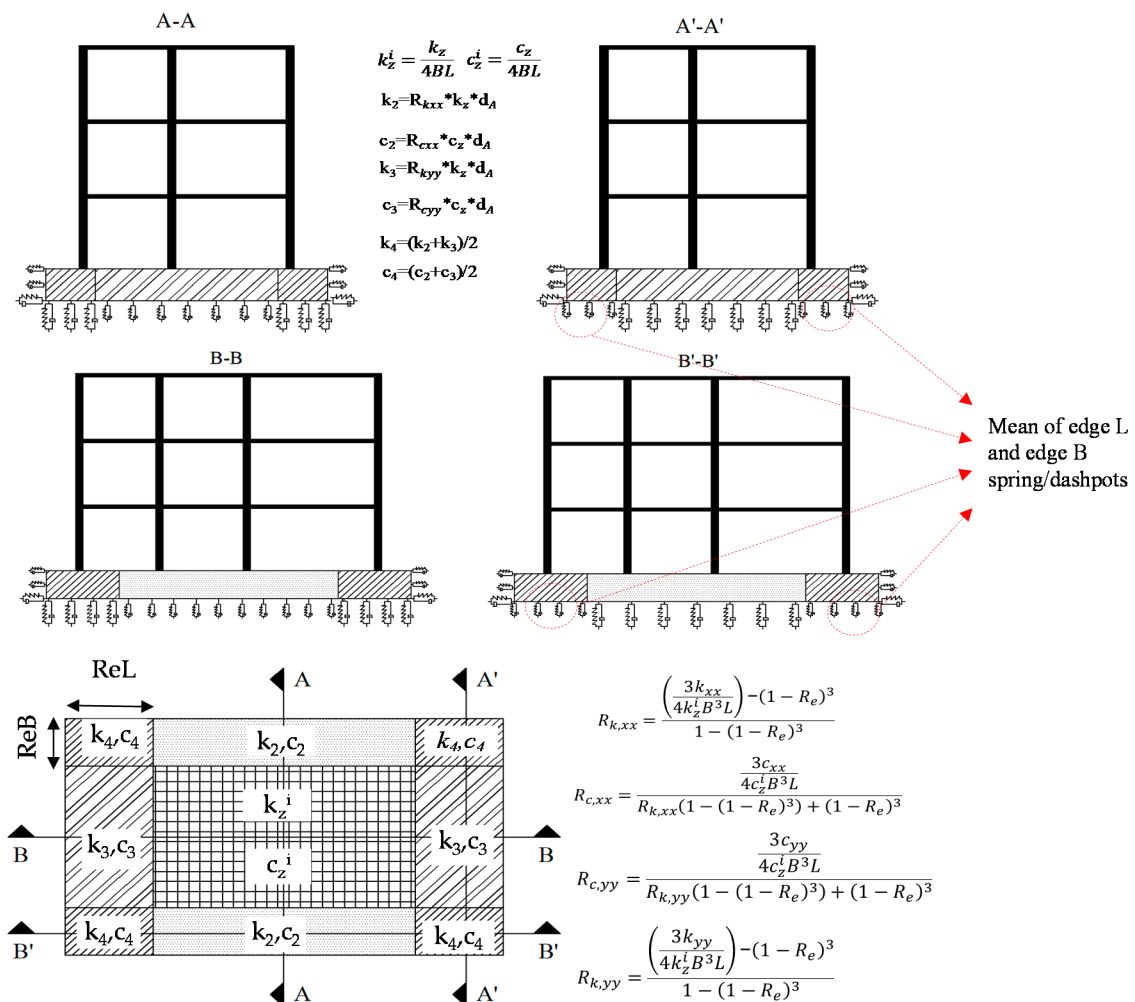$$R_{k,yy} = \frac{\left(\frac{3k_{yy}}{4k_z^i B^3 L}\right) - (1 - R_e)^3}{1 - (1 - R_e)^3}$$

Figure 3. Calculation and representation of stiffness and damping expressions for the foundation springs added to the foundation systems.

Foundation systems of the selected buildings have shallow foundation, and the foundation dimensions were determined according to design projects of the buildings. Both of the base slab averaging and the embedment effects were taken into account by considering soil shear wave velocities, embedment depth of the foundation, and the natural vibration frequencies of structures. The results

indicated that the ground motion reductions (H_u) caused by these effects can be neglected for selected buildings since they can be considered as low- and mid-rise buildings and they have no basement. The values calculated for the embedment effects ($\omega D/V_s$) for all of buildings are lower than 0.006 (Figure 4, left). As a result, the calculated ground motion reduction factors (H_u) are very close to 1 which means that a significant reduction is not needed. A similar situation is also valid for the base slab averaging effects (Figure 4, right). Consequently, obtained results indicate that selected ground motions can directly be used for the nonlinear time history analysis of buildings according to both cases (Figure 4).
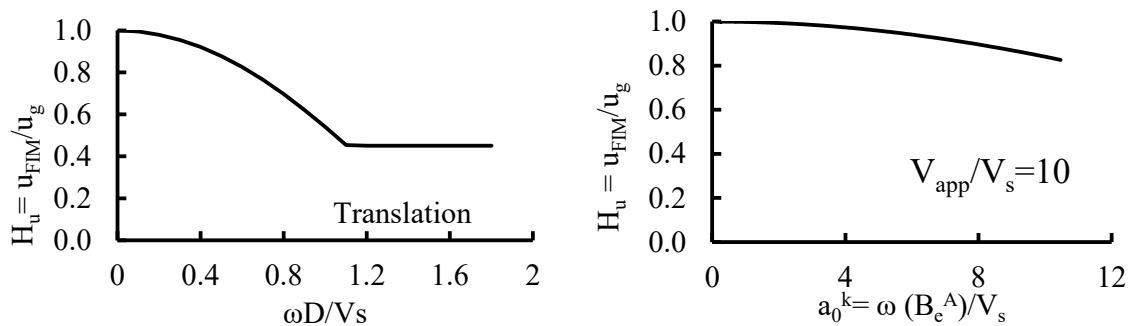
Figure 4. Ground motion reduction factors: (**left**) embedment effects, (**right**) base slab averaging (NIST, 2012).

4. Effect of SSI on the Capacity and Demand Response of Existing Buildings

In this section, capacity-related parameters such as structural period, yield and ultimate (collapse) displacement capacity of members and displacement demands of buildings are evaluated.

4.1. Effect of SSI on the Capacity Curves

All building models were analyzed to determine the capacity curves of buildings according to fixed-based assumption and SSI, and total of 160 (40 buildings × 4 different SSI modeling) analyses were conducted via static pushover analysis. In this paper especially, the "Collapse Prevention" and "Yield" limit states are investigated since one of the purposes of the current study is to determine whether consideration of SSI alters the capacity curves of the buildings.

Collapse prevention damage limits of buildings are determined by checking damage states of columns, beams and the story shear forces. To define building collapse prevention limit, it is assumed that at least 80% of beams in any story should not exceed the member collapse limit. The collapse of any column is accepted as the collapse prevention limit of the buildings. Shear force carried by the columns beyond the yield limit at both ends were checked and the contribution of these columns to the total shear capacity of each story was limited to 30%. Collapse prevention damage limit is determined according to each rule and building damage limit is attained by whichever gives the lowest drift ratio.

After the determination of capacity curves via static pushover analysis, authors investigated whether capacity-related parameters were altered or not when the SSI was considered. Vibration periods (T), ductility capacities (μ) and proportion of drift ratios corresponding to yield, and ultimate damage levels are used to evaluate and compare the effect of SSI on building capacity curves. In order to explain the details of the applied procedure, BO20SN6 was selected among the considered buildings. The first two letters of the building name refer to the design code of the building, and "BO" and "BN" are used to represent old (98−) and new buildings (98+), respectively. The numbers following these letters indicate the order of the building in the inventory. "SN6" refers to the story number of the building. In Figure 5, capacity curve, yield and ultimate damage limits of the BO20SN6 are plotted according to each of the soil classes considered.
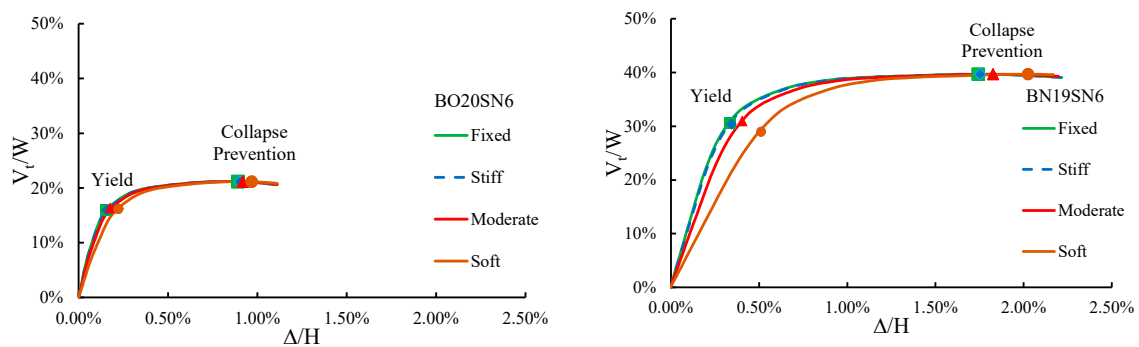
Figure 5. Capacity curves and damage limits of selected old and new buildings.

It can be seen from the figure that yield and ultimate damage levels of the building are shifted left to right from stiff to soft soil types. A similar situation can also be observed for the initial part of the capacity curve. This situation clearly explains the period elongations from stiff to soft soil profiles. It should be stated that similar results were observed for all buildings in the inventory.

In Figure 5, capacity curves of BO20SN6 and BN19SN6 buildings corresponding to different soil conditions are presented. Significant differences between the strength and deformation capacities of selected buildings clearly shows the effect of changing code regulations on the old (98−) and new (98+) buildings. Figure 5 clearly indicates that curves of fixed-base and stiff soil cases are almost identical and capacity curve of moderate soil case is closer to them with respect to the soft soil condition. Variation of capacity curves imply that the main difference occurs in the elastic slope of the building and drift ratios corresponding to yield and collapse limits are significantly affected from SSI in the soft soil case. This figure also indicates that plastic drift capacities of the BO20SN6 building are almost unchanged and the movement of plastic deformation capacity, which is caused by the inertial interaction between structure and soil, can be explained by shifting instead of increasing. Previous studies have also indicated this inertial interaction, and hence elongation of the natural vibration period of the buildings [23].

The studies of Velestos and Nair [24] and Bielak [25] investigated the dimensionless parameters that control the vibration period of the systems in SSI, and they showed that the most important parameter is (h/V_sT), which is known as the structure to soil stiffness ratio. For typical reinforced concrete frame buildings on stiff soil, this ratio is usually less than 0.1 [23]. As this ratio increases, the elongation of the natural vibration period also increases. For this reason, elongation of vibration period resulting from inertial interaction should be taken into consideration when assessing the seismic behavior of structures since the vibration period of the building affects the displacement demand.

The natural period of the buildings in the inventory are determined for each soil type and story groups from the analyses, and mean period values of fixed-base and elongated periods due to different soil classes are shown in Figure 6. Figure 7 also shows that vibration periods increase with increasing story numbers as expected. This situation is valid for all soil types. Comparison of values in Figures 6 and 7 have shown that the elongation of the vibration period is much more significant in the soft soil case and this behavior is identical both in new (98+) and old (98−) buildings (Figure 7).

In addition to vibration periods, elongation of displacement capacities corresponding to yield and collapse limits (as shown in Figure 5) were also investigated for all buildings and soil conditions. Relation between elongation of the vibration periods (T'/T) and change in the yield drift ratios (Δ_y'/Δ_y) depending on the SSI are illustrated in Figure 8. In this figure, T' and Δ_y' notations represent the vibration periods and yield displacements of stiff, moderate and soft soil cases, respectively. T and Δ_y notations, on the other hand, correspond to fixed-base case. Strong correlation between (T'/T) and (Δ_y'/Δ_y) values explains the effect of SSI on the capacity (yield displacement) and demand (period)-related structural parameters of the buildings.

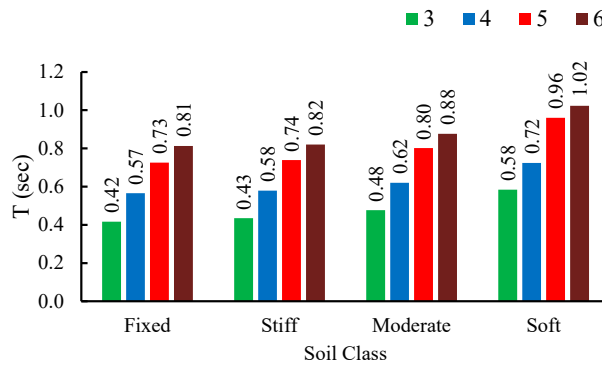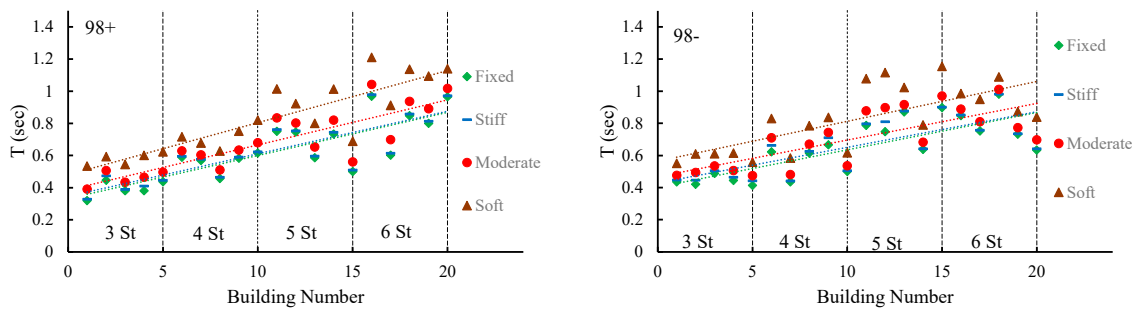**Figure 6.** Distribution of mean vibration periods according to story numbers and soil types.

Figure 7. Distribution of vibration periods for all models according to story numbers and soil types.
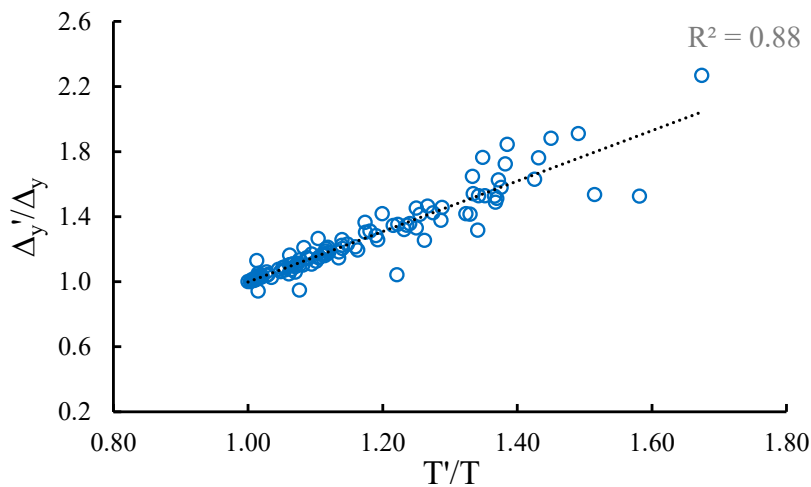

Figure 8. Correlation of shifted yield points and elongated vibration periods.

The effect of SSI on the plastic deformation capacity of buildings is also investigated. For this purpose, plastic drift capacities corresponding to stiff, moderate and soft cases (Δ_p') were divided into the ratios of fixed-base case (Δ_p) and distribution of results is presented in Figure 9. Variation of Δ_p'/Δ_p values indicates that effects of SSI on the plastic deformation capacity of buildings are insignificant and there is no correlation between plastic deformation capacities and period elongations (T'/T) due to SSI.

Effect of this situation can also be examined from the ductility capacities of buildings. Increasing yield displacements and similar plastic drift capacities requires to decrease ductility capacities of buildings. This disadvantage related with the SSI was also reported by Shakib and Homei [26]. In order to investigate the extent of this problem, changes in the ductility ratios depending on the (T'/T) values are presented in Figure 10. Figure 10 clearly shows the considerable decrease in building ductility capacities (μ'/μ) due to effect of SSI [21,22,26].
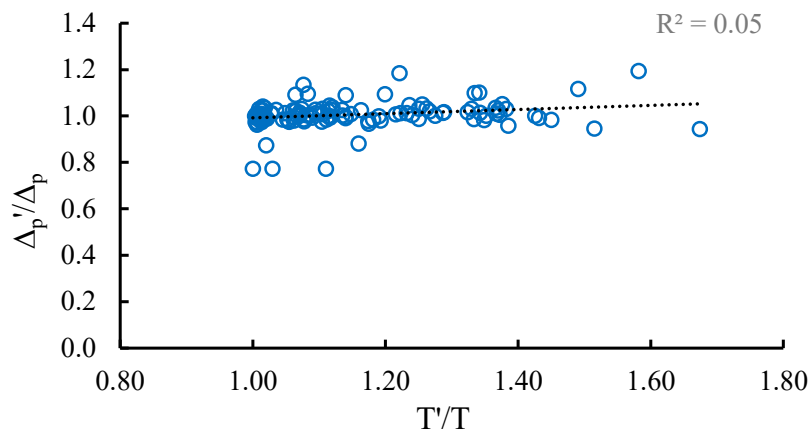
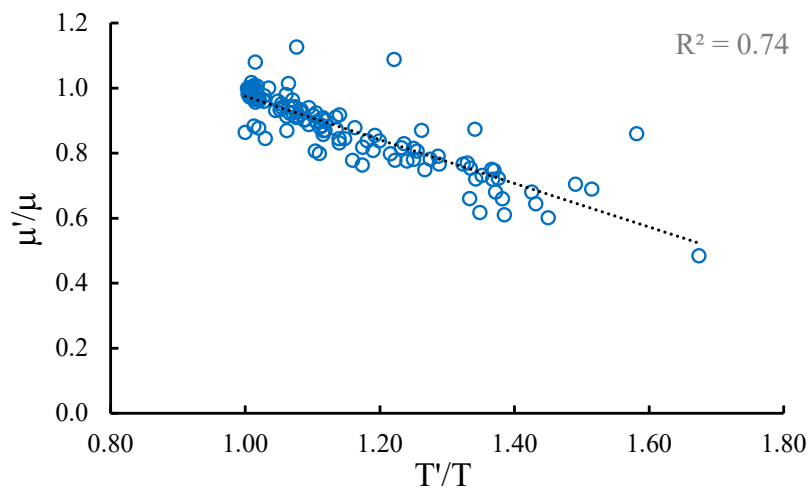**Figure 9.** Correlation of shifted plastic limits and elongated vibration periods.

Figure 10. Decrease in structure ductility capacities with SSI effects.

4.2. Effect of SSI on the Displacement Response of Existing Buildings

To investigate the effect of SSI on the displacement response of buildings, nonlinear dynamic analyses were performed. For this purpose, 20 real strong ground motions were selected [27]. Some attributes of selected records are given in Table 4. Response spectrum of selected records and their mean is drawn in Figure 11. The maximum spectral acceleration of the mean spectrum is around 1.14 g and elastic spectral accelerations are higher than 1 g between the periods of 0.2 s to 0.6 s.

Effect of SSI on the displacement response of existing buildings was investigated by two different earthquake demand parameters (EDPs): roof and inter-story drift ratios. Roof displacement is one of the most widely used parameters and it has wide applicability, especially for determining the seismic performance of structures. However, seismic performance of buildings is determined according to different seismic intensity or earthquake levels. Different earthquake levels can be recommended for different performance levels according to building importance in the modern seismic codes. Earthquake levels, on the other hand, are described according to different exceeding probability levels. Considering this situation, roof drift demand ratios of existing buildings are investigated in a probabilistic manner. For this purpose, cumulative exceedance probability of drift ratios is calculated from the displacement demands of buildings which are subjected to 20 real earthquake records. In order to generalize obtained results, cumulative exceeding probabilities are provided for different building groups (new and old), story numbers and soil type which are modeled according to the substructure method.

Table 4. General properties of selected real earthquake records.

Name of Acceleration	Depth (km)	PGA (g)	PGV (cm/s)	PGD (cm)	V_{max}/A_{max} (s)
CAP-RIO270	18.50	0.39	40.58	47.44	0.11
CHI-TCU74N	13.67	0.35	39.54	49.12	0.12
CHI-TCU95W	43.44	0.38	59.39	80.09	0.16
COA-PLE045	8.50	0.59	59.38	14.36	0.10
KOC-DZC270	12.70	0.36	61.02	252.44	0.17
LAN-CLVTR	21.20	0.42	41.40	22.07	0.10
LOM-BRN000	10.30	0.45	50.43	16.20	0.11
LOM-BRN090	10.30	0.50	43.79	13.03	0.09
LOM-CYC285	21.80	0.48	43.91	81.28	0.09
LOM-G03090	14.40	0.37	43.08	25.31	0.12
LOM-SAR000	13.00	0.51	41.26	16.42	0.08
NOR-CNP196	15.80	0.42	57.01	67.59	0.14
NOR-LOS000	13.00	0.41	44.84	20.16	0.11
NOR-LOS270	13.00	0.48	44.52	15.25	0.09
NOR-MU2035	20.80	0.62	41.93	16.57	0.07
NOR-MUL009	19.60	0.42	55.74	55.98	0.14
NOR-ORR090	22.60	0.57	53.72	37.60	0.10
NOR-ORR360	22.60	0.51	51.32	31.36	0.10
NOR-SAT180	13.30	0.48	65.88	102.17	0.14
NPAL-NPS210	8.20	0.59	72.12	13.45	0.12
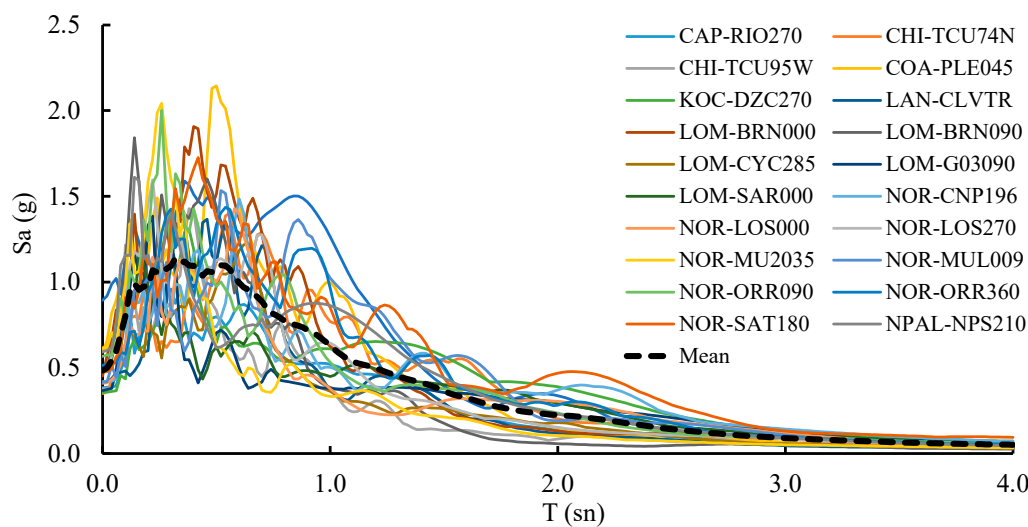
Figure 11. Response spectrum of selected real ground motion records used in this study.

In order to determine cumulative probability of exceedance curves, maximum displacement demands of each building at roof level were determined and these demands were collected in the data pool. In each data pool 100 drift ratios (5 buildings × 20 acceleration records) corresponding to each story group of new and old buildings were obtained and then they were ranked from minimum to maximum. Minimum and maximum values in the data pool represent the drift ratios corresponding probability of exceeding 100% and 0%, respectively. In order to compare the drift demands between the fixed-base and SSI approaches, different exceedance probability levels were also considered. For this purpose, drift ratios corresponding to probability of exceeding 50% and 10% levels were used. Cumulative exceedance probabilities of three- to six-story buildings are plotted in Figures 12–15. It can be seen from the figures that roof drift probabilities of the fixed-base approach and stiff soil conditions are very similar, and they are mostly overlapped. Drift demands of moderate soil condition are closer to fixed-base and stiff soil cases with respect to soft soil condition. These figures clearly show that roof

demands gradually increase due to SSI, and the most significant effect of SSI is observed on soft soil case in all story groups of new and old buildings.
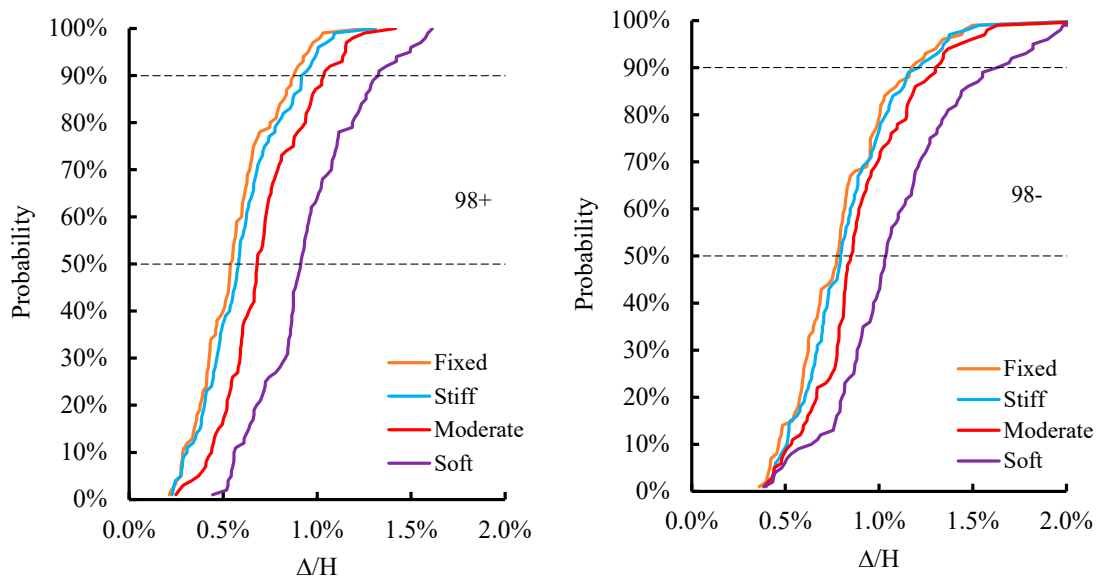

Figure 12. Cumulative exceedance probability curves of the three-story buildings.
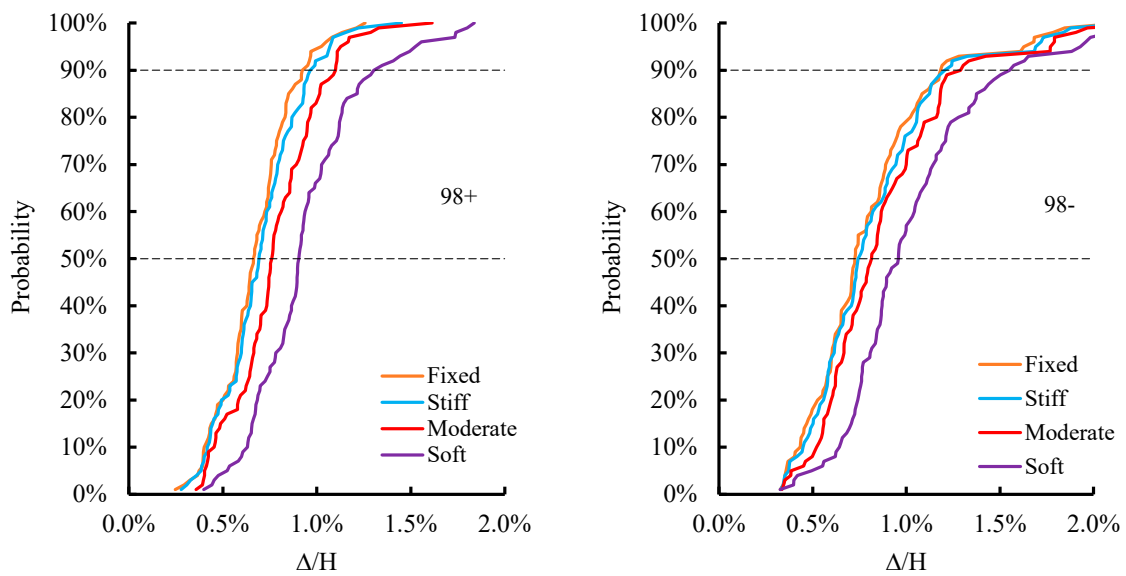

Figure 13. Cumulative exceedance probability curves of the four-story buildings.
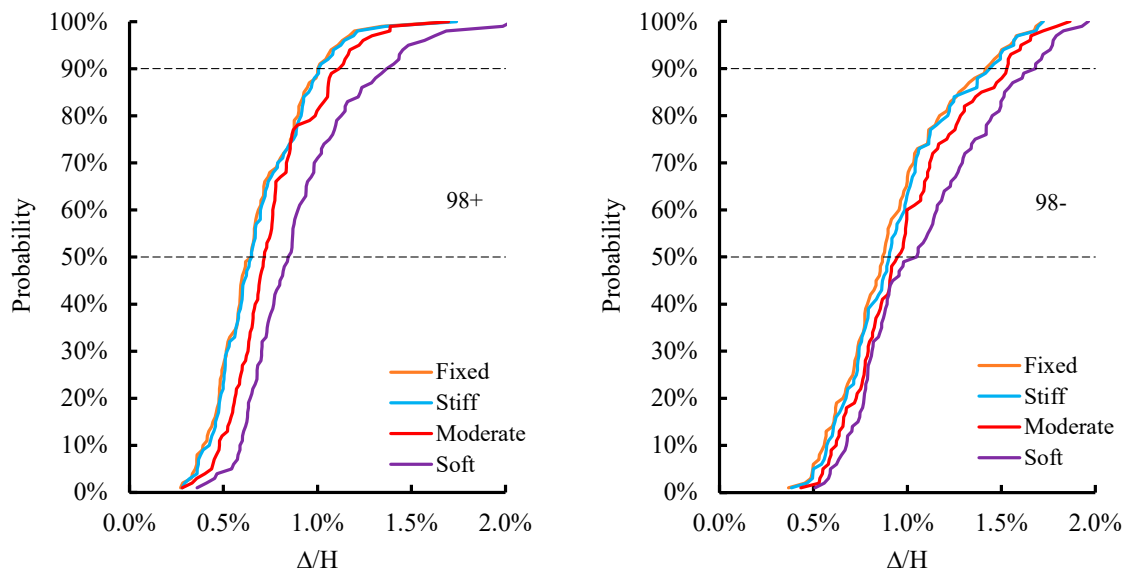
Figure 14. Cumulative exceedance probability curves of the five-story buildings.
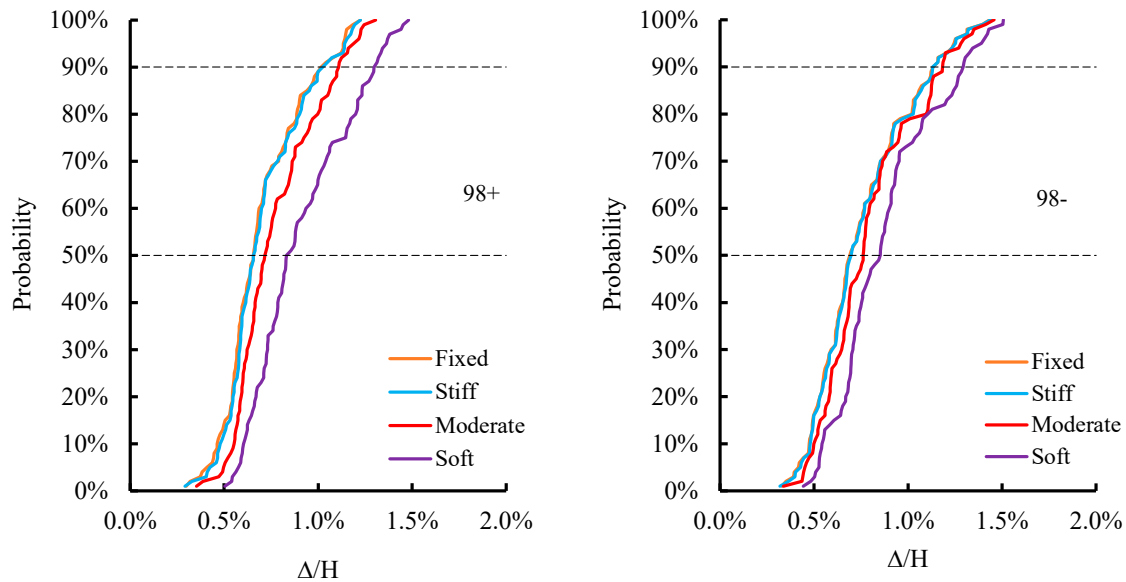

Figure 15. Cumulative exceedance probability curves of the six-story buildings.

Distribution of results also shows that probabilistic roof displacement demands in old buildings (98−) are greater than new ones (98+), as expected. On the other hand, differences among the roof demand curves of especially in five- and six-story buildings are relatively low with respect to other ones. In other words, the effect of SSI is much more pronounced in low-rise buildings having relatively higher stiffness capacities and strength ratios. This situation is much more evident in three- and four-story new buildings (98+). All these investigations have shown that relative effect of SSI especially in soft soil case is much more significant in stiffer and stronger buildings.

Numerical evaluations of results have indicated that probabilistic roof drift ratios calculated for soft soil case can be 1.3 to 1.7 times greater than that of fixed-base case in three-story new buildings. However, these ratios decrease to 1.2 to 1.3 in three-story old buildings depending on the probability of exceeding levels (50%, 10% and maximum (0%)). The same ratios in six-story old buildings range from 1.05 to 1.2. These numerical comparisons indicate that the relative effect of SSI is much more effective in stiffer and stronger low-rise buildings. It can be admitted that the obtained results show consistency with the results obtained from similar studies in literature [21].

In addition to evaluation of roof drift ratios, effects of SSI on the inter-story drift ratios are also discussed. In Figures 16–23, mean inter-story drift ratios are plotted for different building groups and soil types. While calculating the inter-story drift ratios, the same method was applied. One hundred inter-story drift ratios obtained from five buildings and 20 acceleration records were used and values corresponding to probability of exceeding levels of 50%, 10% and maximum drift ratios were averaged. This method was repeated for each story group. Variation of inter-story drift ratios clearly show that the most significant changes depending on the SSI occur at the bottom stories of the buildings [21] and the most evident increments are again observed in the soft soil case. All of these figures indicate that inter-story drift ratios are increased in the soft soil case in all probability levels. Inter-story drift ratios at 50% probability level are lower than 0.5% and the difference between the soil types in terms of story drift ratios is not obvious.
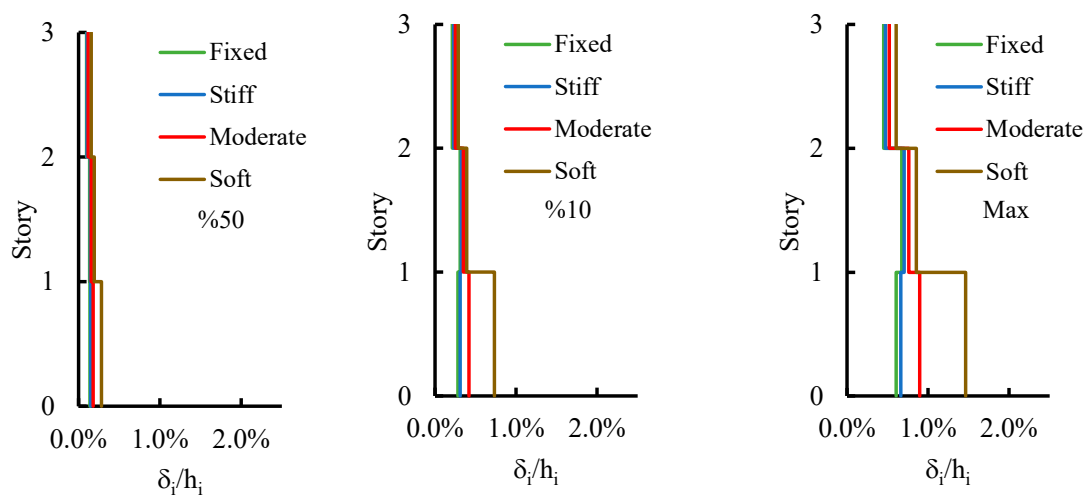

Figure 16. Mean of inter-story drift ratios corresponding to different exceedance probability levels for three-story new buildings.
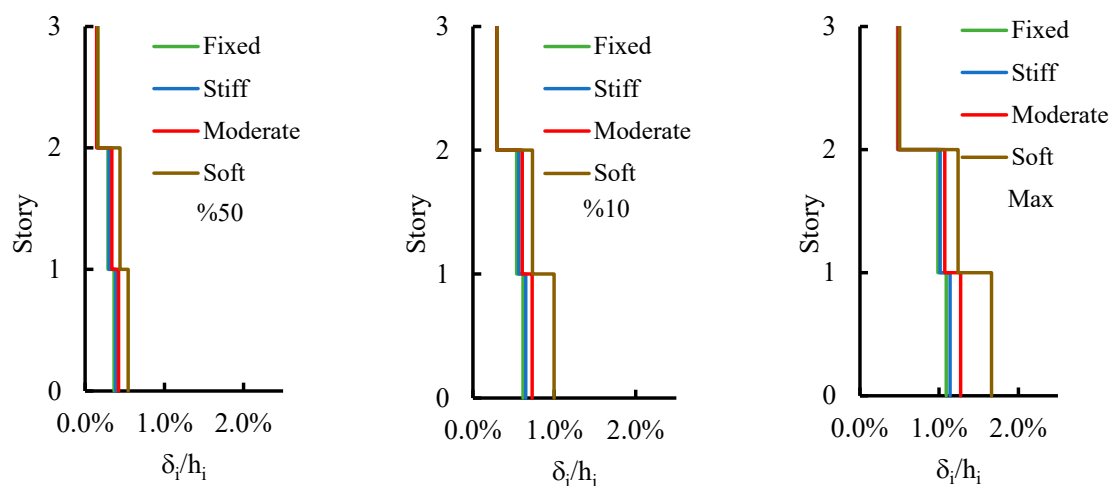

Figure 17. Mean of inter-story drift ratios corresponding to different exceedance probability levels for three-story old buildings.
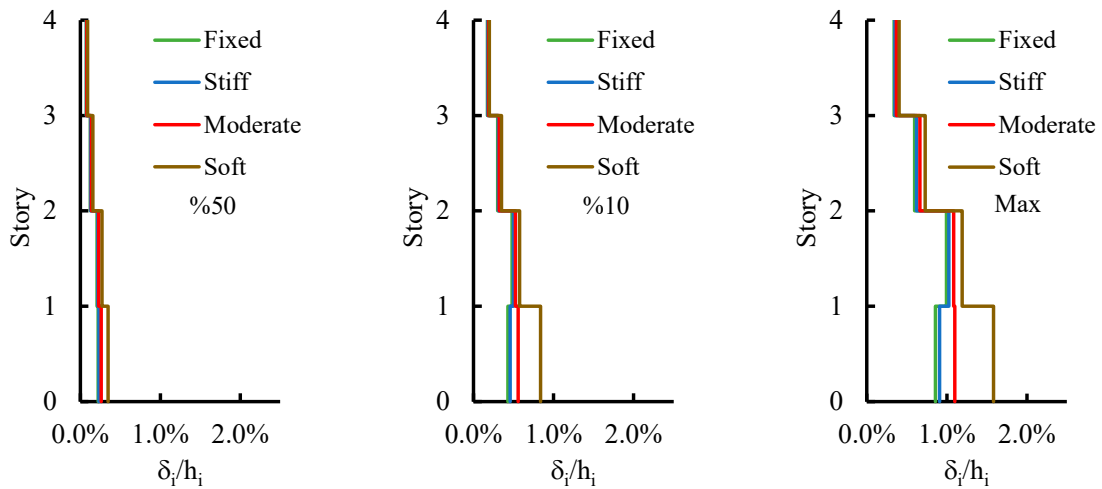
Figure 18. Mean of inter-story drift ratios corresponding to different exceedance probability levels for the four-story new buildings.
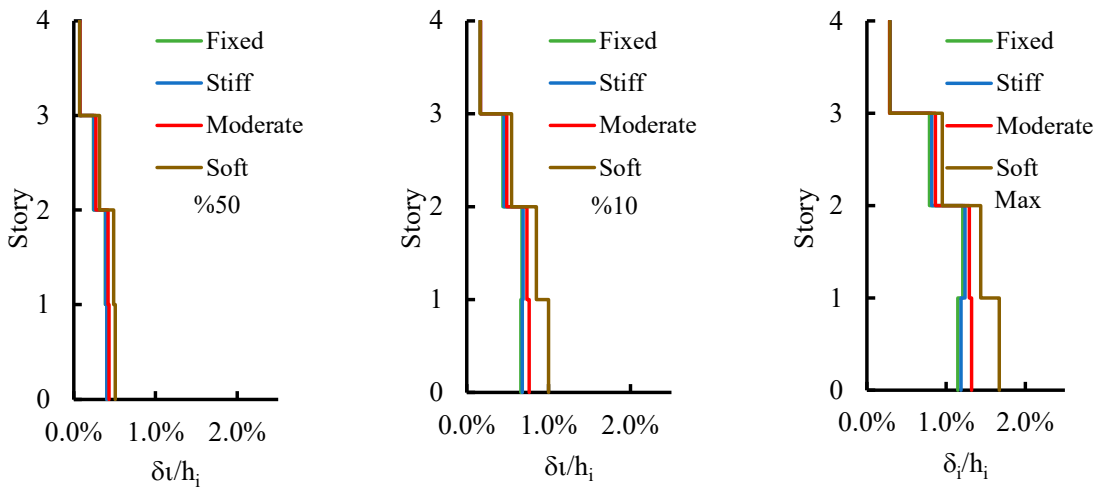

Figure 19. Mean of inter-story drift ratios corresponding to different exceedance probability levels for the four-story old buildings.
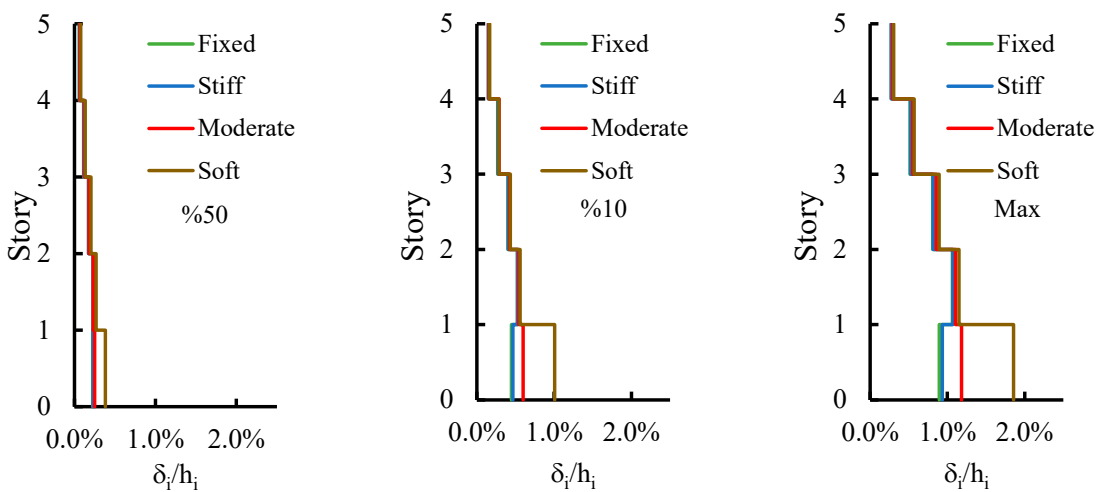

Figure 20. Mean of inter-story drift ratios corresponding to different exceedance probability levels for the five-story new buildings.
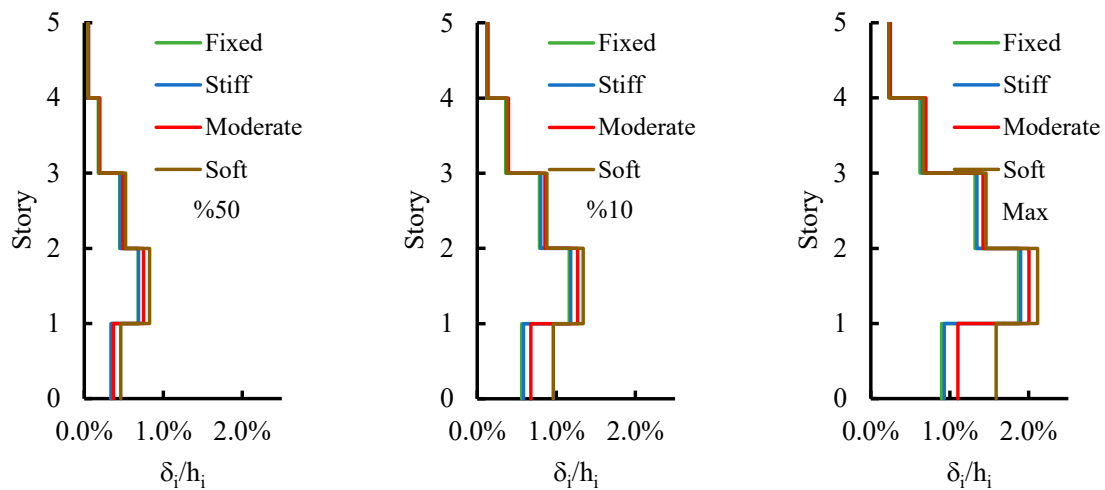
Figure 21. Mean of inter-story drift ratios corresponding to different exceedance probability levels for the five-story old buildings.
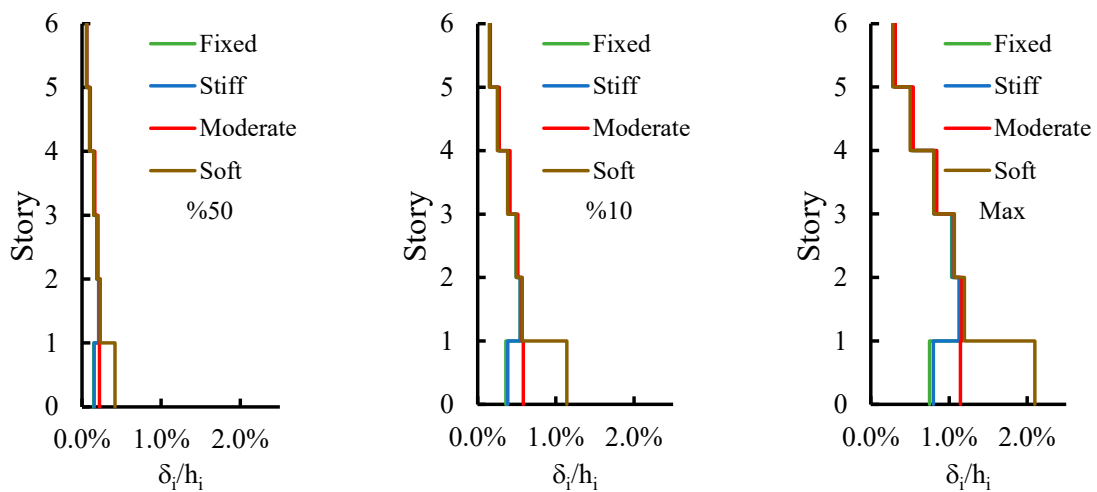

Figure 22. Mean of inter-story drift ratios corresponding to different exceedance probability levels for the six-story new buildings.
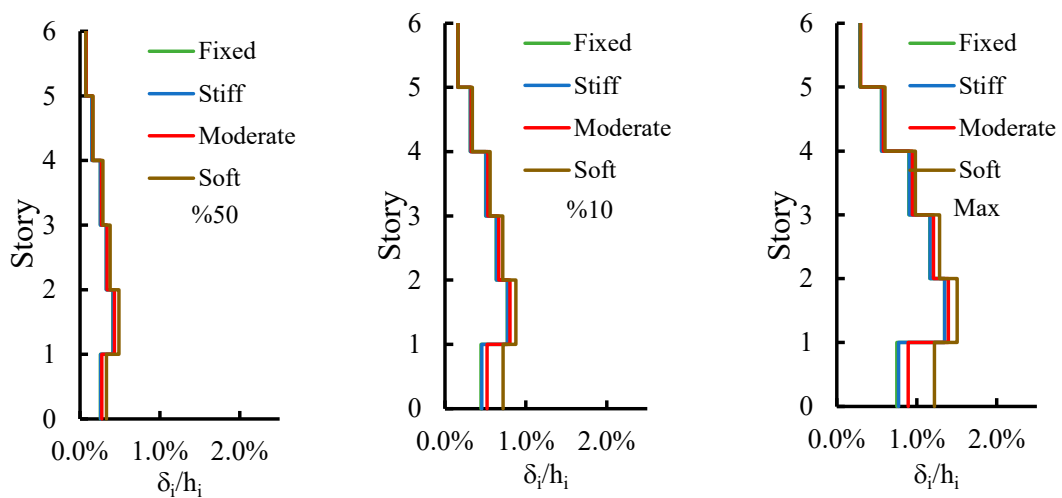

Figure 23. Mean of inter-story drift ratios corresponding to different exceedance probability levels for the six-story old buildings.

Drift ratios corresponding to probability of exceeding 10% are higher than that of 50% ratios and the effect of SSI becomes more apparent. Inter-story drift ratios at this probability level can be close to 1% in soft soil cases. However, variations of drift demands have indicated that the effect of SSI is not significant in upper stories and the response of upper stories is limited with respect to bottom stories. This situation is similar for all building groups and soil conditions. At this point, it should be stated that drifts caused by the rotations at the base due to SSI were extracted while calculating the inter-story drift ratios of first stories.

Distribution of values indicates that the inter-story drift ratios of stiff and moderate soil conditions are closer to the fixed-base case with respect to ratios of soft soil. Story drifts corresponding to the soft soil case are much more remarkable and the level of increment is much more pronounced with respect to other cases. These observations about the effect of soil conditions are compatible with the findings related to the probabilistic roof drift ratios presented in Figures 12–15.

Comparisons of probabilistic inter-story drift ratios indicate that there are considerable differences among the maximum and other probabilistic drift ratios. Effect of SSI is much more evident on the maximum drift ratios and results have shown that maximum drifts can approximately be greater than four times from the 50% drifts and two times from the 10% drifts. Graphical distributions show that these trends are almost similar in old (98−) and new (98+) buildings, but differences among the probabilistic drift demands are quite significant.

Maximum inter-story drift ratios of buildings resting on soft soils are mostly higher than 1.5% and maximum inter-story drift ratios are generally accumulated at the first stories. This situation is much more apparent in low-rise buildings (three- and four-story) independent from the building group. However, distribution of values has shown that drift demands of especially upper stories are higher in old buildings with respect to new ones (see Figures 21 and 23). Critical stories in five- and six-story old buildings are the second stories and SSI does not change this situation. Decrease in column dimensions in the upper stories and the relatively higher vibration periods caused by upper stories are more critical in old buildings (98−). However, in new buildings the SSI strongly affected the response of first stories and the place of the critical story moved to the first story. The ratio of increment is much more significant in the first stories of new buildings with respect to old ones.

5. Comparison of SSI Effects on the Seismic Performance of Existing Buildings

Obtained results clearly show that interaction between soil and the structure affects both calculation of displacement capacities and demands in existing buildings. This situation implies that seismic performance of these buildings should also be examined since the performance is determined by comparing both capacity and demand.

Calculation of capacity curves revealed that interaction between soil and the structure shifts the total displacement capacity of buildings instead of increasing them. Assessments performed after pushover analyses show that plastic deformation capacity of buildings remains almost constant (Figure 9) while yield displacements increase. Decreasing displacement ductilities corresponding to soft soils are the indicator of this situation (Figure 10). Changes in the elastic slope of the building capacity curves also imply the elongations in vibration periods and hence higher seismic displacement demands in buildings (Figure 5). Figures 12–15 clearly represent this increase in demands from stiff to soft soil sites. All these capacity- and demand-related changes in the results are the indicator of possible seismic performance changes in selected buildings.

Seismic performance of investigated buildings was determined by using Turkish Earthquake Code regulations and the effect of SSI on the collapse risk of old and new buildings was compared. At this point, it should be reminded again that the aim of this study is not to investigate the seismic performance of selected buildings according to one specific code regulations. The aim of this study is to understand whether consideration of SSI can change the capacity and demand calculations (and hence the performance estimations) of existing buildings. For this reason, the number of collapsed buildings under various soil conditions was determined and compared.

In Turkish Earthquake Code, seismic performance of buildings is determined by using strain-based damage assessment method. Furthermore, accumulation of damages, whether in beams or columns, contributes to damaged columns and the shear capacity of stories are additional factors which are considered by the Turkish Earthquake Code for the seismic performance assessment. In Figure 24, changes in the number of collapsed buildings located on stiff to soft soil sites are presented. Increasing damage trends show that interaction between soil and the structure is much more significant, especially in soft soils, and a number of collapsed buildings on soft soils sites are considerably higher than that of others. Figure 24 also reveals that the devastating effects of SSI are much more evident in old buildings with respect to new ones. Higher seismic capacities of new constructions (Figure 5) suppress the deteriorating effects of SSI and the effect of interaction becomes limited on new buildings.
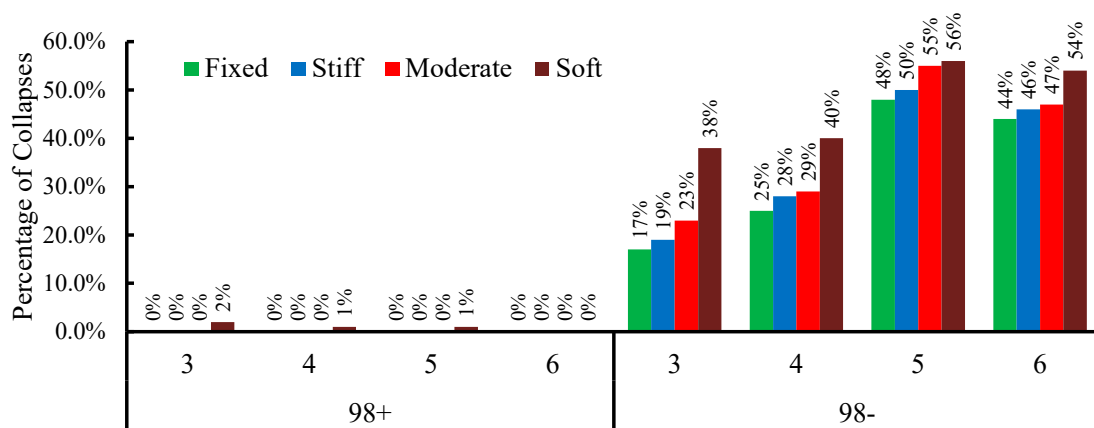

Figure 24. Distribution of number of collapse events for the existing buildings (%).

Figure 24 also shows that in each soil condition seismic performance of old buildings decreases by the increasing number of stories. However, the ratio of collapsed buildings on soft soil to fixed-base case indicates that the relative effect of SSI is much more significant in lower story buildings. In three-story old buildings the ratio of collapsed buildings on soft soils (38%) is greater than two times that of the fixed-base case (17%). Differences between soft and moderate soil cases are much more apparent with respect to moderate and stiff or stiff and fixed-base cases.

Distribution of collapsed buildings is presented in Figure 24 and these values clearly show that seismic performance of especially older constructions is significantly affected from the SSI. Results have clearly revealed that damage risk significantly increases in soft soil cases with respect to moderate and stiff cases.

6. Conclusions

Forty existing buildings constructed before and after in 1998 when the modern seismic design code of Turkey was implemented were investigated by considering soil-structure interaction. Seismic response of buildings was determined by using non-linear time history analyses and 20 strong ground motions. Interaction between soil and the structure was modeled by applying the substructure method and four different cases classified according to shear wave velocities were considered. Seismic displacement demands at roof and story levels were calculated for all buildings under fixed-base, stiff, moderate and soft soil conditions.

In addition to demand calculations by using non-linear time history analyses, capacity curves of the buildings were obtained through static pushover analyses. By this method, drift ratios corresponding to yield and ultimate levels were obtained for each soil case and for each building. Then, displacement demands and building capacities were investigated, the effects of soil-structure interaction on existing buildings under various soil conditions were compared and the results are summarized below.

The capacity curves obtained from the static pushover analyses of old and new buildings show that the interaction between soil and the structure shifts the total displacement capacity of buildings instead of increasing it. Depending on the weak soil conditions, rotations at base increase and this situation increases the elastic drift ratios corresponding to the yield. In other words, plastic deformation capacity of buildings remains almost constant while yield displacements increase. Decreasing displacement ductilities are the result of this situation. Changes in the elastic slope of the buildings also increase the vibration periods and then the displacement demands of the buildings.

Changes in the seismic demands were investigated by comparing the roof drift ratios corresponding to exceedance probabilities of 50%, 10% and maximum. Distribution of values clearly indicated that most critical results were obtained under soft soil conditions, and results obtained from the soft soil cases were significantly separated from the others. Drift demands of moderate soil cases are closer to fixed and stiff soil cases with respect to soft soil conditions. Relative demand increase under soft soil case is much more evident in low story buildings with respect to higher ones.

Investigation of inter-story drift demands showed that first stories are mostly affected from the weak soil conditions and in all cases most significant demand increase occurs at the first stories. Increase in the maximum inter-story drift demand is much more evident with respect to ones corresponding to 50% and 10% exceedance probabilities.

Effect of soil conditions on the number of collapsed buildings is also investigated and compared. Distribution of results have shown that a number of collapsed buildings are almost similar in fixed-base, stiff and even in moderate soil cases. However, under soft soil conditions the number of collapsed buildings increase and the level of increment is much more significant in old and low story buildings. A distinct increase in the number of collapsed three- and four-story buildings indicates that the fragility of old and low story buildings on weak soil conditions is much higher. Performance of new buildings, on the other hand, is not as critical as the old ones. Higher seismic capacities of new constructions suppress the deteriorating effects of soft soil conditions and reduce the collapse risk of new buildings.

Author Contributions: S.M.S. conceived of the presented idea, supervised the work, and drafted the manuscript. M.P. contributed to method of analysis and supervised the analytical computations. A.K. and I.O. designed the nonlinear structural models and analyzed the buildings. All authors have read and agreed to the published version of the manuscript.

References

1. National Institute of Standards and Technology (NIST); National Earthquake Hazards Reduction Program. *GCR 12-917-21 Soil-Structure Interaction for Building Structures*; National Institute of Standards and Technology: Gaithersburg, MD, USA, 2012.

2. Federal Emergency Management Agency (FEMA). *Recommended Seismic Provisions for New Buildings and Other Structures*; FEMA P-750-1/2009; Federal Emergency Management Agency (FEMA): Washington, DC, USA, 2009.

3. Federal Emergency Management Agency (FEMA); National Earthquake Hazards Reduction Program. *Improvement of Nonlinear Static Seismic Analysis Procedures*; FEMA 440; Federal Emergency Management Agency (FEMA): Washington, DC, USA, 2005.

4. American Society of Civil Engineers ASCE. *Seismic Evaluation and Retrofit of Existing Buildings*; ASCE/SEI 41-06; American Society of Civil Engineers: Reston, VA, USA, 2007.

5. Shehata, E.; Ahmed, M.M.; Alazrak, T.M.A. Evaluation of soil structure-interaction effects of seismic response demands of multi-story MRF buildings on raft foundations. *Int. J. Adv. Struct. Eng.* **2015**, *7*, 11–30.

6. Mylonakys, G.; Gazetas, G. Seismic soil-structure interaction: Beneficial or detrimental? *J. Earthq. Eng.* **2000**, *4*, 277–301. [CrossRef]

7.   Federal Emergency Management Agency (FEMA); National Earthquake Hazards Reduction Program. *Recommended Seismic Provisions for New Buildings and Other Structures*; FEMA P-1050-1/2015; Federal Emergency Management Agency (FEMA): Washington, DC, USA, 2015.

8.   Kausel, E. Early history of soil-structure interaction. *Soil Dyn. Earthq. Eng.* **2010**, *30*, 822–832. [CrossRef]

9.   Gazetas, G. Formulas and charts for impedances of surface and embedded foundations. *J. Geotech. Eng.* **1991**, *117*, 1363–1381. [CrossRef]

10.   Mylonakys, G.; Nikolaou, S.; Gazetas, G. Footings under seismic loading: Analysis and design issues with emphasis on bridge foundations. *Soil Dyn. Earthq. Eng.* **2006**, *26*, 824–853. [CrossRef]

11.   Fatahi, B.; Tabatabaiefar, H.R.; Samali, B. Performance based assessment of dynamic soil-structure interaction effects on seismic response of building frames. In Proceedings of the GeoRisk 2011: Geotechnical Risk Assessment and Management, Atlanta, GA, USA, 26–28 June 2011; pp. 344–351.

12.   Turkish Earthquake Code, TEC-2007. *Specifications for Buildings to Be Built in Seismic Areas*; Ministry of Public Works and Settlement: Ankara, Turkey, 2007.

13.   Turkish Building Earthquake Code, TBEC-2018. *Turkish Earthquake Code: Specifications for Building Design Under Earthquake Effects*; Ministry of Public Works and Settlement: Ankara, Turkey, 2018.

14.   Kalkan, A. Estimation of Probabilistic Seismic Hazard Risk and Earthquake Insurance Rates in Existing Reinforced Concrete Buildings. Ph.D. Thesis, Institute of Science Department, Pamukkale University, Denizli, Turkey, 2019.

15.   Turkish Earthquake Code, TEC-1998. *Specifications for Buildings to be Built in Seismic Areas*; Ministry of Public Works and Settlement: Ankara, Turkey, 1998.

16.   Scot, B.D.; Park, R.; Priestley, M.J.N. Stress-strain behavior of concrete confined by overlapping hoops at low and high strain rates. *J. Am. Concr. Inst.* **1982**, *79*, 13–27.

17.   Palanci, M.; Kalkan, A.; Senel, S.M. Investigation of shear effects on the capacity and demand estimation of RC buildings. *Struct. Eng. Mech.* **2016**, *60*, 1021–1038. [CrossRef]

18.   Pais, A.; Kausel, E. Approximate formulas for dynamic stiffness of rigid foundations. *Soil Dyn. Earthq. Eng.* **1998**, *7*, 213–227. [CrossRef]

19.   Tan, C.G.; Majid, T.A.; Ariffin, K.S.; Bunnori, N.M. Effects of site classification on empirical correlation between shear wave velocity and standard penetration resistance for soils. *Appl. Mech. Mater.* **2013**, *284–287*, 1305–1310. [CrossRef]

20.   Pitilakis, K.; Riga, E.; Anastasiadis, A. New code site classification, amplification factors and normalized response spectra based on a worldwide ground-motion database. *Bull. Earthq. Eng.* **2013**, *11*, 925–966. [CrossRef]

21.   Raychawdhury, P. Seismic response of low-rise steel moment-resisting frame (SMRF) buildings incorporating nonlinear soil–structure interaction (SSI). *Eng. Struct.* **2011**, *33*, 958–967. [CrossRef]

22.   Tahghighi, H.; Mohammadi, A. Numerical evaluation of soil-structure interaction effects on the seismic performance and vulnerability of reinforced concrete buildings. *Int. J. Geomech.* **2020**, *20*, 04020072. [CrossRef]

23.   Stewart, J.P.; Seed, R.B.; Fenves, G.L. Seismic soil-structure interaction in buildings. II: Empirical findings. *J. Geotech. Geoenviron. Eng.* **1999**, *125*, 38–48. [CrossRef]

24.   Veletsos, A.S.; Nair, V.V. Seismic interaction of structures on hysteretic foundations. *J. Struct. Eng.* **1975**, *101*, 109–129.

25.   Bielak, J. Dynamic behavior of structures with embedded foundations. *Earthq. Eng. Struct. Dyn.* **1975**, *3*, 259–274. [CrossRef]

26.   Shakib, H.; Homaei, F. Probabilistic seismic performance assessment of the soil structure interaction effect on seismic response of midrise setback steel buildings. *Bull. Earthq. Eng.* **2017**, *15*, 1827–2851. [CrossRef]

27.   Pacific Earthquake Engineering Center (PEER). PEER Ground Motion Database. Available online: https://ngawest2.berkeley.edu/ (accessed on 21 June 2019).

Publisher's Note: MDPI stays neutral with regard to jurisdictional claims in published maps and institutional affiliations.